World Academy of Science, Engineering and Technology
International Journal of Environmental and Ecological Engineering
Vol:18, No:9, 2024

Measurement Uncertainty Evaluation of Meteorological Model: CALMET

N. Miklavčič, U. Kugovnik, N. Galkina, P. Ribarič, R. Vončina

***Abstract*—**Today the need for weather predictions is deeply rooted in the everyday life of people as well as it is in industry. The forecasts influence final decision-making processes in multiple areas from agriculture and prevention of natural disasters to air traffic regulations and solutions on a national level for health, security, and economic problems. Namely in Slovenia, alongside other existing forms of application, weather forecasts are adopted for the prognosis of electrical current transmission through powerlines. Meteorological parameters are one of the key factors which need to be considered in estimations of the reliable supply of electrical energy to consumers. And like for any other measured value, the knowledge about measurement uncertainty is critical also for the secure and reliable supply of energy. The estimation of measurement uncertainty grants us a more accurate interpretation of data, a better quality of the end results, and even a possibility of improvement of weather forecast models.

***Keywords*—**Measurement uncertainty, microscale meteorological model, CALMET meteorological station, orthogonal regression.

I. Introduction

IN today's interconnected world, weather forecasting has become an indispensable part of our daily lives. It is utilized for both personal and economic purposes. For personal use, it serves to protect oneself and one's property, and to plan leisure activities. In the realm of economic activities, forecasts impact decision-making processes in various fields, ranging from agriculture and natural disaster prevention to the regulation of air traffic and the solutions at the national level for health, safety, and economic issues.

Weather prediction is dependent on numerous factors, including geographic location, topography, atmospheric conditions, and human influence. Therefore, the forecast is always an approximation and carries a certain degree of measurement uncertainty.

Understanding the measurement uncertainty in meteorological forecasts enables a more reliable use and interpretation of the meteorological models themselves, enhancing the credibility and applicability of the predictions. Measurement uncertainty aids in identifying potential deviations and errors, leading to improved strategies for risk management and enhancing the reliability of weather forecasting.

This article will focus on a specific aspect of meteorological forecasting - the assessment of measurement uncertainty of meteorological parameters obtained with the diagnostic microscale meteorological model CALMET. With a deeper understanding of this uncertainty, we will gain a better interpretation of the model's results, which will contribute to the accuracy of weather predictions and thus refine the reliability of meteorological forecasts as a whole.

II. Method

To determine the measurement uncertainty of meteorological parameters was configured a set up for a simulation with the diagnostic microscale meteorological model CALMET. Furthermore, 31 meteorological stations with sensors providing temporally consistent data were deployed.

The measurement uncertainty was then calculated from an annual dataset for temperature, wind speed, relative humidity, and solar radiation. The determination of measurement uncertainty is based on a comparison between measured and predicted values and includes the measurement uncertainty of the used equipment, the uncertainty of systematic errors, and the uncertainty resulting from deviations between measured and predicted values.

A. Microscale Meteorological Model CALMET

For the purpose of calculating atmospheric conditions, the diagnostic meteorological model CALMET version 6.327 is used. The settings of the program followed the recommendations of USEPA applied in version V5.8.5, which was officially certified by the USEPA on July 26, 2016 [1]. CALMET is designed for the preparation of a three-dimensional meteorological field over rugged and complex terrain at a local spatial scale [2]. In combination with the CALPUFF model, it has been developed for modelling the dispersion of pollutants in the outdoor air. [3].

CALMET allows to include prognostic and observed meteorological data in the diagnostic wind-field module in three different ways:

- The first method uses only meteorological stations without the results of the mesoscale meteorological model.
- The second method utilizes results from the mesoscale meteorological model without including meteorological stations.
- The third method is a combination of results from the mesoscale meteorological model with meteorological stations.

CALMET reconstructs three-dimensional wind and temperature fields in its forecasts, deriving from meteorological

N. M., U. K., and N. G. are with the Milan Vidmar Electric Power Research Institute, 1000 Ljubljana, Slovenia (phone: 003861-474-36-01; e-mail: nina.miklavcic@eimv.si, urska.kugovnik@eimv.si, natalia.galkina@eimv.si).

P. R. is with the Meteorološke in ekološke storitve,Primož Ribarič s.p., 2311 Hoce, Slovenia (phone: 0038631-269-294; e-mail: primozribaric@gmail.com).

measurements, orography, and land use data. It determines two-dimensional fields of meteorological variables needed for dispersion simulation and calculates phenomena such as coastal and slope winds, atmospheric stability, and turbulence intensity. The calculation of wind fields employs a two-stage approach. In the first step, the wind field obtained from the prognostic model is adjusted to the terrain, slopes, and potential obstacles, which is then weighted in the second step by considering any entered measured or observed meteorological data

In our CALMET simulations we handled input data using third method, where prognostic data were introduced like a replacement for the initial guess wind field at step one and 31 meteorological stations distributed across Slovenia were treated as observational data to produce a second step result wind field.

B. Input data

The input data used to determine atmospheric conditions with the CALMET model include:

- Mesoscale meteorological data obtained from the ALADIN simulations, nested in the global forecast ensemble ECMWF. In Slovenia provider of mentioned datasets is Slovenian Environment Agency ARSO (Agencija Republike Slovenije za okolje). These data include forecasts of atmospheric conditions with a 1-hour resolution for the next 72 hours. The vertical resolution of the forecast ensemble is 48 layers with 4.4 km grid spacing. The parameters included in dataset are: vertical velocity, pressure, cumulative precipitation, cumulative solar radiation, temperature, u and v wind speeds, and relative humidity for each layer.
- CALMET data from ALADIN model, downscaled to 8 vertical layers with the size of domain 5 km and resolution 100 m.
- Terrain data from the Shuttle Radar Topography Mission (SRTM) collection with a resolution of 90 meters [4].

The description of land-use is expected to be detailed and relatively up to date in order to better reflect meteorology and dynamics in atmosphere in complex terrain. Land-cover is directly related to surface roughness, which influences the development of the vertical wind profile. For this purpose, CORINE land cover data from 2018 were included, which differentiate among 44 classes of various land uses with horizontal resolution of 100 m [5]. In this way we satisfied the requirement of finer or equal resolution between land use data and grid-spacing of model.

C. Meteorological Data from Measurement Stations

Wind speed, temperature, and relative humidity measurements were conducted using a Vaisala device, model WXT 536. Solar radiation measurements were collected with a device from Kipp & Zonen, model SMP6. Meteorological sensors were installed on power line poles at a height of 10 meters above the ground. The quality of the measurements was ensured through regular maintenance, calibrations, and by providing traceability of all relevant activities related to the measurement systems. The data are owned by ELES, d. o. o., the operator of the combined transmission and distribution power network in Slovenia, who permitted the use of this data. Locations are shown on Fig. 1.

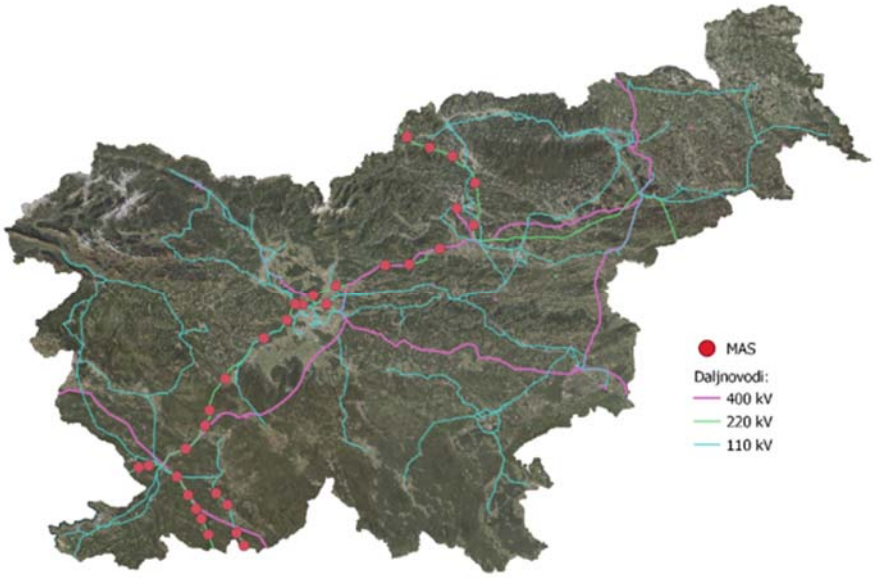

Fig. 1 Location of stations MAS

D. Calculation of Combined Measurement Uncertainty

To calculate the combined measurement uncertainty of each meteorological parameter, we identified the sources of uncertainty contributions along with their probability distributions, determined or calculated the magnitudes of each contribution, and the inter-correlations of individual influential

quantities. To ensure an equal level of confidence for all contributions to the measurement uncertainty, each contribution was transformed into a standard measurement uncertainty as required.

The combined measurement uncertainty is composed of uncertainties arising from the measurement equipment, its installation, and the uncertainties of systematic error (u_{BIAS}) and deviations (u_{RT}), which stem from differences between data obtained from model estimates and measured values. The uncertainty of the measurement equipment includes multiple contributions, that vary from one measured parameter to another. These contributions are summarized based on the manufacturer's specifications and certificates.

Measurement uncertainties, resulting from deviations of individual measurements (u_{RT}) and from systematic differences (u_{BIAS}), are based on the comparison between measured values from meteorological stations at specific locations and model-derived values using the third method. Both contributions consider the temporal synchronization of data and the measurement location. The measured values serve as a reference in this context. The forecasted model values of meteorological parameters using the third method will henceforth be referred to by the acronym GWD.

In determining u_{RT} and u_{BIAS}, we started with the assumption that the relationship between the measured values at meteorological stations and the model-derived values can be described by a linear equation (1), where the coefficients of the linear function, y_i (a and b) are the model-derived results, and x_i are the measured values.

$$y_i = \mathrm{a} + \mathrm{b}x_i \tag{1}$$

In the linear relationship between two variables, the method of least squares, which seeks the best linear fit between the two variables, can be used to determine measurement uncertainty [6]. However, in cases like ours, where the values measured at meteorological stations also have measurement errors, a special case of the least squares method, called orthogonal regression, can be applied. This method takes into account the errors in both variables to achieve a more accurate fit and estimation of measurement uncertainty [7], [8].

The method of orthogonal regression is deployed to adjust the estimate of predictor errors. Unlike simple linear regression it accounts for a computational error in answer and the predictor. In this context, model-derived values and measurements are considered. Orthogonal regression approach performs linear adjustment by minimizing the sum of squares of differences between the two variables, taking into account the variability of both variables. It is used when it is necessary to fit a linear function between the variables while simultaneously considering errors in both variables for a more accurate estimation of fitting and measurement uncertainty.

E. Uncertainty of Deviation Resulting from Individual Measurements

Measurement uncertainty, brought by deviations of individual measurements u_{RT} is calculated using (2) [9]:

$$\mathrm{u}_{RT}^2(y_i) = \frac{RSS}{(n-2)} + [\mathrm{a} + (\mathrm{b}-1)x_i]^2 \tag{2}$$

where $u_{RT}(y_i)$ represents the uncertainty of the GWD results, *RSS* is the sum of residuals arising from orthogonal regression, n is the number of samples, x_i are the measured values from the meteorological station, and a and b are the coefficients of the linear function. The sum of residuals, *RSS*, arising from orthogonal regression is calculated using (3) [9]:

$$RSS = \sum_{i=1}^{n}(y_i - a - bx_i)^2 \tag{3}$$

The algorithm used to calculate the parameters a and b for orthogonal regression is expressed in formulas from (4)-(10) [9].

Calculation of the Slope b:

$$b = \frac{S_{yy} - S_{xx} + \sqrt{(S_{yy} - S_{xx})^2 + 4(S_{xy})^2}}{2S_{xy}} \tag{4}$$

where x_i is the value measured by meteorological stations and y_i is the modelled value obtained from GWD:

$$S_{xx} = \sum_{i=1}^{N_{ux}}(x_i - \bar{x})^2\, b \tag{5}$$

$$S_{yy} = \sum_{i=1}^{N_{ux}}(y_i - \bar{y})^2 \tag{6}$$

$$S_{xy} = \sum_{i=1}^{N_{ux}}(x_i - \bar{x})(y_i - \bar{y}) \tag{7}$$

$$\bar{x} = \frac{\sum_{i=1}^{N_{ux}} x_i}{N_{ux}} \tag{8}$$

$$\bar{y} = \frac{\sum_{i=1}^{N_{ux}} y_i}{n} \tag{9}$$

Calculation of the initial value a (10):

$$\mathrm{a} = \bar{y} - b\bar{x} \tag{10}$$

F. Uncertainty BIAS

BIAS uncertainty refers to the uncertainty associated with the system's or method's deviation from the reference value. BIAS results from systematic errors, that lead to systematic deviations of the results from the true value.

BIAS uncertainty is calculated based on (11):

$$u_{BIAS}(y) = a + (b-1)MV \tag{11}$$

In (11), a and b represent the initial value and the slope obtained through orthogonal regression. MV represents the value of the individual parameter. BIAS uncertainty depends on the actual value of the measured or predicted parameter and varies accordingly.

For the parameters:

- Temperature,
- Wind speed,
- Relative humidity, and
- Solar radiation

The combined measurement uncertainty for the predicted model values of GWD has been calculated. Contributions to the measurement uncertainty are listed below, separated for each influencing parameter.

G. Temperature Measurement Uncertainty

The combined measurement uncertainty of temperature is composed of contributions arising from the measurement equipment, summarized based on the manufacturer's specifications, calibrations, and uncertainties resulting from differences between meteorological measurements and predicted values from GWD. The combined measurement uncertainty for temperature, $u_c(T)$, is calculated using (12) and includes the following contributions:

- uncertainty of accuracy from the reference method $u_{sp,T}$,
- uncertainty of resolution from the reference method $u_{r,T}$,
- calibration uncertainties of the reference method $u_{c,T,}$
- uncertainty based on systematic difference (BIAS) $u_{BIAS,T}$ and
- uncertainties due to deviations in GWD $u_{RT,T}$

When determining the measurement uncertainty of temperature obtained from model estimates, there is no correlation between individual quantities, therefore the sensitivity coefficient c_T is equal to one.

$$u_c(T) = \sqrt{c_T^2(u_{sp,T}^2 + u_{r,,T}^2 + u_{c,T}^2 + u_{BIAS,T}^2 + u_{RT,T}^2)} \quad (12)$$

H. Relative Humidity Measurement Uncertainty

The combined measurement uncertainty of relative humidity is composed of contributions arising from the measurement equipment, summarized based on the manufacturer's specifications, calibrations, and uncertainties resulting from differences between meteorological measurements and predicted values from GWD. The combined measurement uncertainty for relative humidity, $u_c(RH)$ is calculated using (13) and includes the following contributions:

- uncertainty of accuracy from the reference method $u_{sp,RH}$,
- uncertainty of resolution from the reference method $u_{r,RH}$,
- calibration uncertainties of the reference method $u_{c,RH,}$
- uncertainty based on systematic difference (BIAS) $u_{BIAS,RH}$ and
- uncertainties due to deviations in GWD $u_{RT,RH}$

$$u_c(RH) = \sqrt{c_{\mathrm{rh}}^2(u_{sp,\mathrm{RH}}^2 + u_{r,\mathrm{RH}}^2 + u_{c,\mathrm{RH}}^2 + u_{BIAS,\mathrm{RH}}^2 + u_{RT,\mathrm{RH}}^2)} \quad (13)$$

I. Measurement Uncertainty of Wind Speed

The combined measurement uncertainty for wind speed, $u_c(v)$, is composed of contributions arising from the measurement equipment, as summarized based on the manufacturer's specifications, calibrations, and uncertainties resulting from differences between meteorological measurements and predicted values from GWD. The combined measurement uncertainty for wind speed is calculated using (14) and includes the following contributions:

- uncertainty of accuracy from the reference method, $u_{sp,v}$,
- uncertainty of resolution from the reference method, $u_{r,v}$,
- calibration uncertainties of the reference method, $u_{c,v,}$
- uncertainty based on systematic differences (BIAS) $u_{BIAS,v}$ and
- uncertainties due to deviations in GWD, $u_{RT,v}$

$$u_c(v) = \sqrt{c_v^2(u_{sp,v}^2 + u_{r,v}^2 + u_{c,v}^2 + u_{BIAS,v}^2 + u_{RT,v}^2)} \quad (14)$$

J. Measurement Uncertainty of Solar Radiation

The combined measurement uncertainty of solar radiation is composed of contributions arising from the measurement equipment, summarized according to the manufacturer's specifications, calibrations, and uncertainties resulting from differences between meteorological measurements and the predicted values (GWD). The combined measurement uncertainty for solar radiation, $u_c(S)$, is calculated using (15) and includes the following contributions:

- uncertainty due to zero offset of the reference method $u_{ZERO,S}$,
- uncertainty due to drift of the reference method $u_{D,S}$,
- uncertainty due to nonlinearity of the reference method $u_{L,S,}$
- uncertainty due to temperature response of the reference method $u_{T,S,}$
- uncertainty due to the angle of incidence of the sun $u_{S,S,}$
- uncertainty due to spectral selectivity of the reference method $u_{ss,S}$,
- uncertainty due to tilt of the reference method $u_{TR,S}$,
- uncertainty due to resolution of the reference method $u_{r,S}$,
- calibration uncertainties of the reference method $u_{c,S,}$
- uncertainty based on systematic difference (BIAS) $u_{BIAS,S}$ and
- uncertainties due to deviations in GWD $u_{RT,S,}$

$$u_c(v) = \sqrt{\begin{matrix} c_S^2(u_{ZERO,S}^2 + u_{L,S}^2 + u_{T,S}^2 + u_{S,S}^2 + u_{ss,S}^2 \\ +u_{TR,S}^2 + u_{r,S}^2 + u_{c,S}^2 + u_{BIAS,v}^2 + u_{RT,v}^2) \end{matrix}} \quad (15)$$

K. Probability Distributions of Individual Contributions

Uncertainty due to the resolution of the measuring instrument, denoted as $u_{r,T}$, $u_{r,RH}$, $u_{r,v}$ and $u_{r,S}$ is included in all considered meteorological parameters and is summarized according to the specifications of the measurement equipment [10], [11]. The uncertainty of resolution is provided with a lower and upper limit and due to its contribution, needs to be divided by $\sqrt{12}$. Other contributions summarized from the specifications of the measurement equipment, such as $u_{sp,T,}$ $u_{sp,RH,}$ $u_{sp,v,}$ $u_{ZERO,S}$, $u_{S,S,}$, $u_{D,S}$, $u_{L,S}$, $u_{T,S}$, $u_{ss,S}$ $u_{TR,S}$ are distributed according to a rectangular probability distribution and need to be divided by $\sqrt{3}$.

Calibration uncertainty, denoted as $u_{c,T,}$ $u_{c,RH,,}$ $u_{c,v,}$ in $u_{c,S,}$ is summarized from the calibration certificate [12], [13], which indicates a normal distribution (expanded measurement uncertainty $k = 2$). This contribution should be divided by 2.

The standard uncertainties of systematic error BIAS $u_{BIAS,T.}$ $u_{BIAS,RH,}$ $u_{BIAS,v}$ *or* $u_{BIAS,S}$ and the uncertainties resulting from deviations of individual measurements, $u_{RT,T,}$ $u_{RT,RH,}$ $u_{RT,v}$ *or* $u_{RT,S}$ are calculated using (2) and (11).

The calculated combined standard measurement uncertainty

for each parameter provides a result with a 68.3 % confidence level. However, to achieve a higher confidence level, at least 95 %, the obtained results are multiplied by a factor of $k = 2$ (16):

$$U_{(95\%)}(y) = k \cdot u_c(y) \quad (16)$$

III. Results

The calculated expanded measurement uncertainty with a confidence interval of 95.5% is based on the annual data set from 2022. The results of the expanded measurement uncertainty for each parameter obtained with the microscale meteorological model CALMET, incorporating meteorological stations (GWD), are presented in Figs. 2-9.

A. Temperature

In Figs. 2 and 3, the expanded measurement uncertainty of temperature is presented. Fig. 2 shows the calculated measurement uncertainty for each station at 15 °C. The differences between individual locations are clearly visible from the graph. Fig. 3 illustrates the measurement uncertainty for the entire measured area. The line on the graph represents the average measurement uncertainty of temperature, derived from the calculated uncertainties at all stations. The area chart depicts the minimum and maximum measurement uncertainties for individual temperature values.

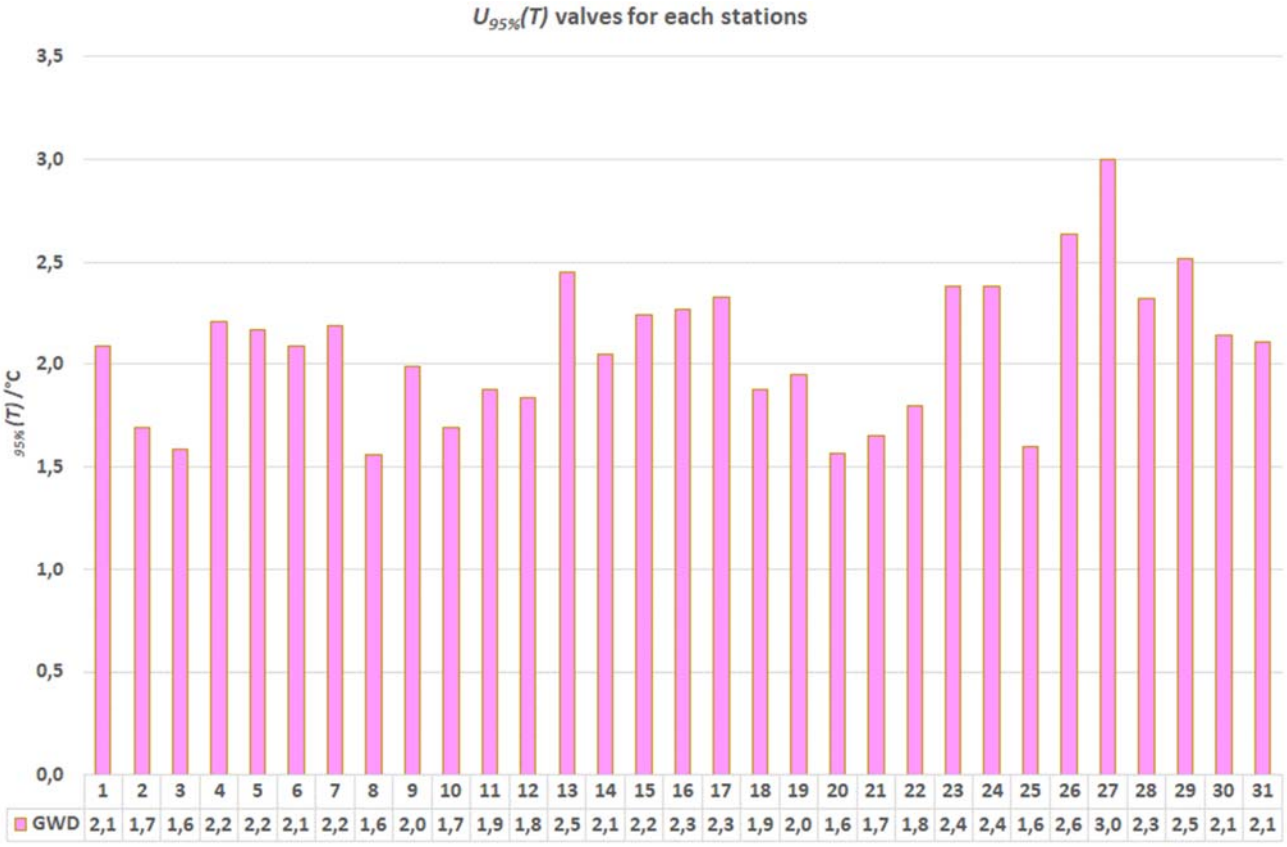

Fig. 2 Expanded measurement uncertainty $U_{95\%}(T)$ at T = 15 °C calculated for each meteorological station

B. Relative Humidity

In Figs. 4 and 5, the expanded measurement uncertainty for relative humidity is illustrated. Fig. 4 presents the calculated uncertainty for each station at 80 %RH, where the differences between the various locations are clearly noticeable. Fig. 5 depicts the measurement uncertainty across the entire measured area. The line on the graph indicates the average uncertainty for relative humidity, which is derived from the uncertainties at all stations. The area chart shows the range of minimum and maximum uncertainties for individual relative humidity values.

C. Wind Speed

In Figs. 6 and 7, the expanded measurement uncertainty for wind speed is shown. Fig. 6 displays the uncertainty calculated for each station at 4 m/s, clearly revealing the differences between the locations. Fig. 7 provides an overview of the uncertainty across the entire measured area. The line on the graph indicates the average uncertainty for wind speed, which is based on the calculated uncertainties from all stations. The area chart illustrates the range between the minimum and maximum uncertainties for specific wind speed values.

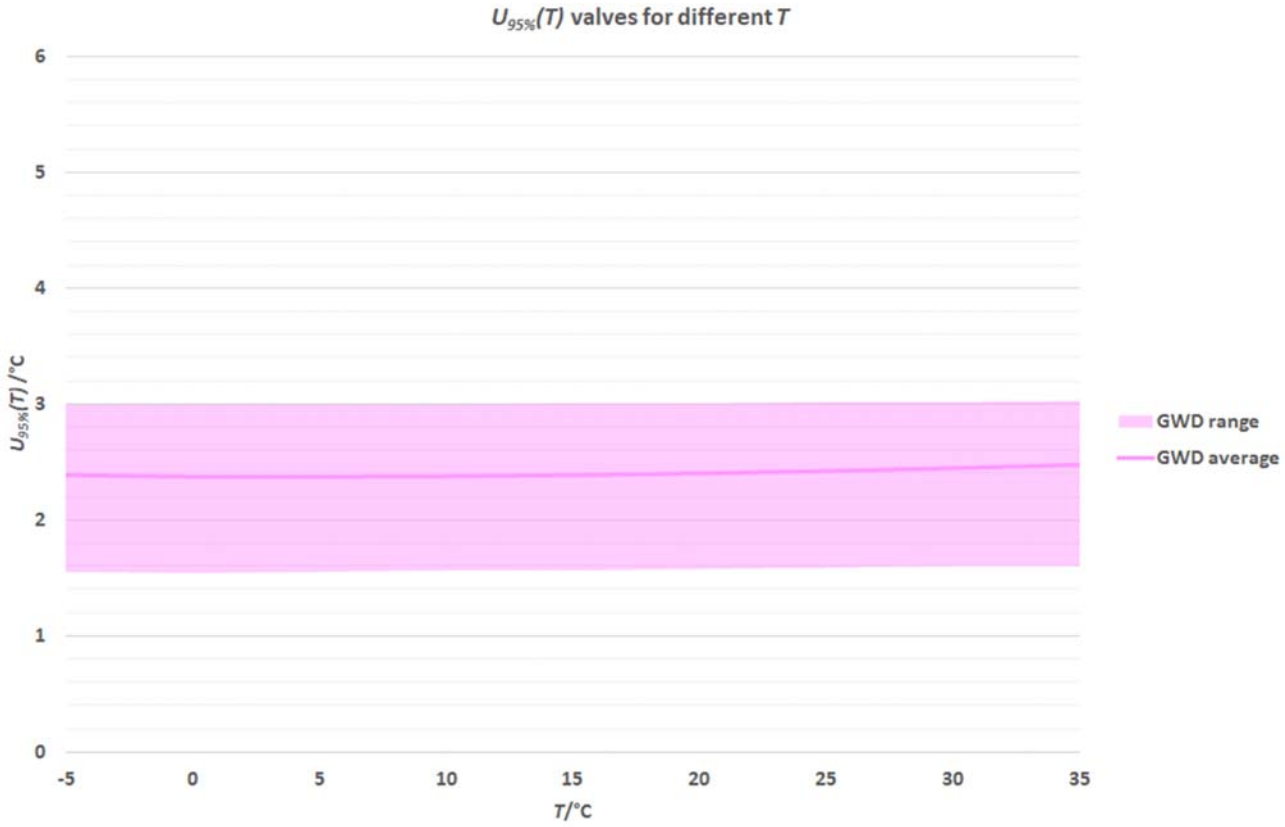

Fig. 3 Expanded measurement uncertainty $U_{95\%}(T)$ at various values of T (line chart - average measurement uncertainty; area graph - range of measurement uncertainties)

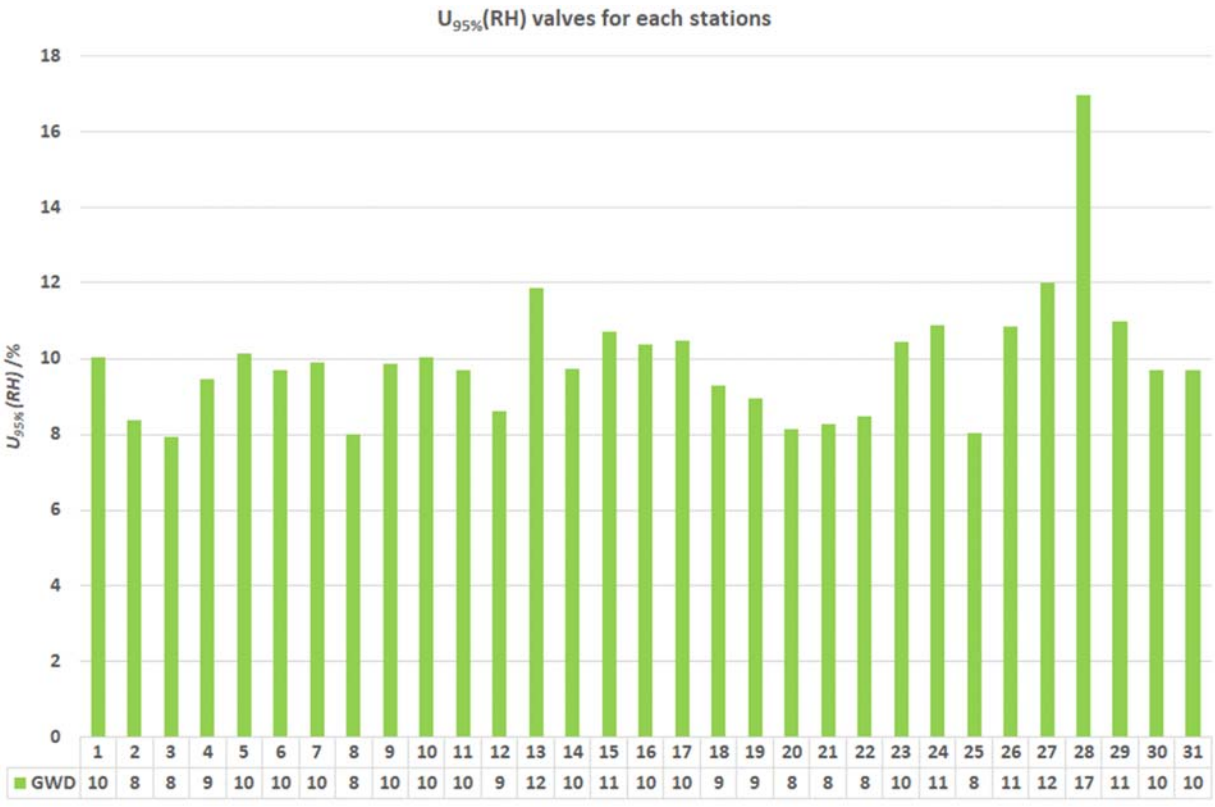

Fig. 4 Expanded measurement uncertainty $U_{95\%}(RH)$ at RH = 80% calculated for each station

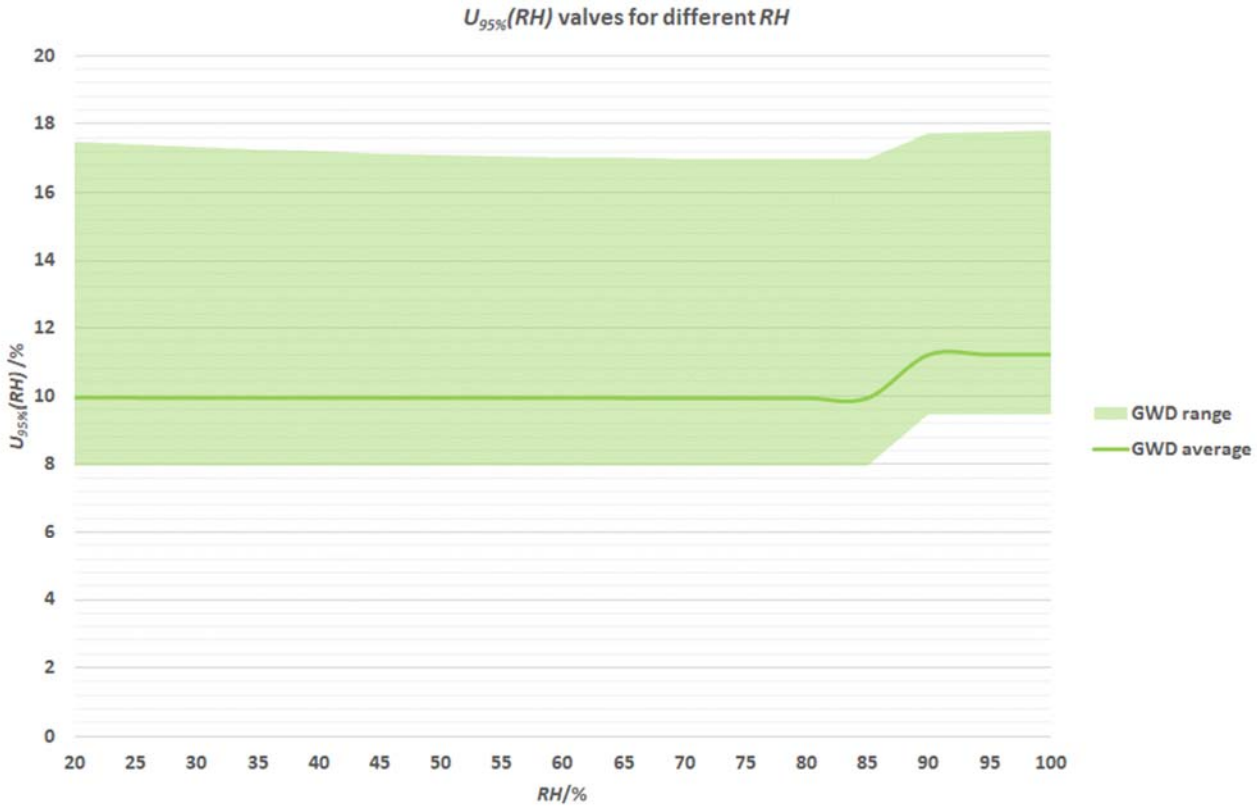

Fig. 5 Expanded measurement uncertainty $U_{95\%}(RH)$ at various values of RH (line chart - average measurement uncertainty; area graph - range of measurement uncertainties)

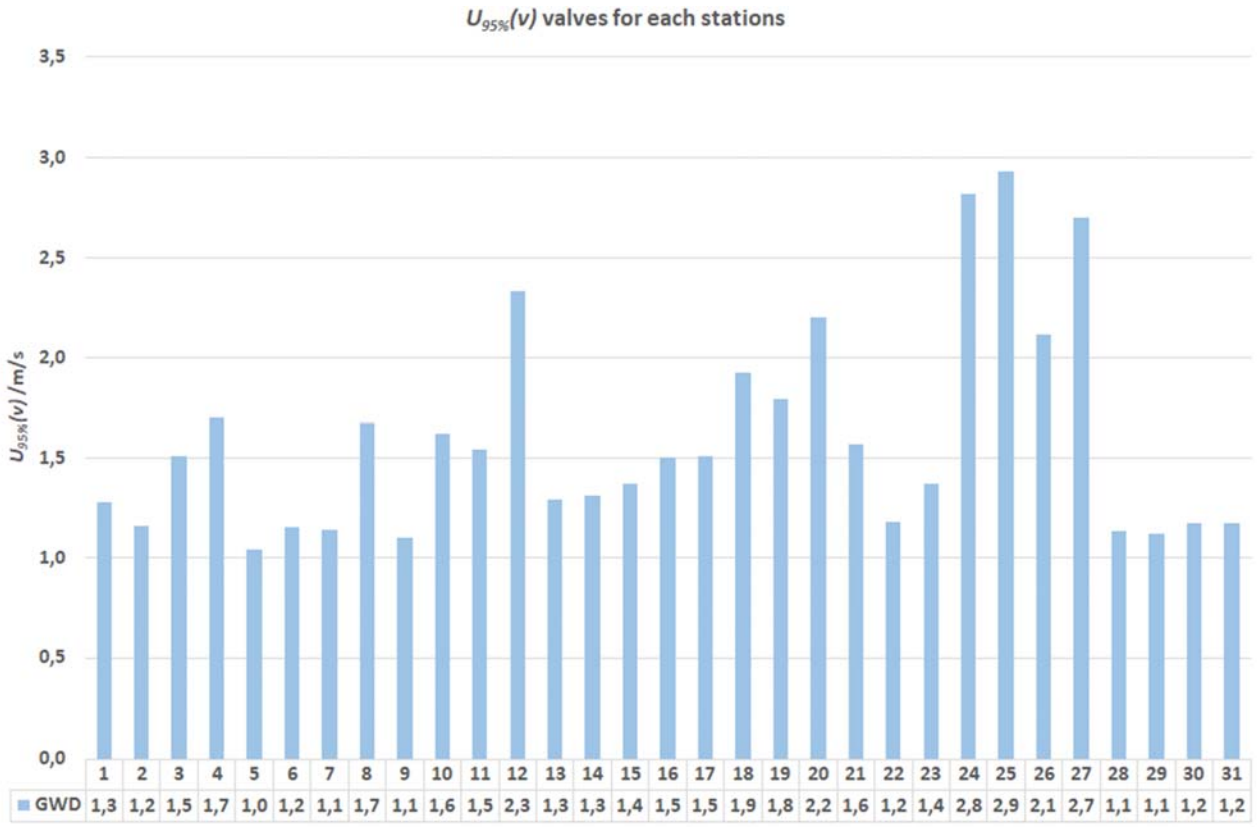

Fig. 6 Expanded measurement uncertainty $U_{95\%}(v)$ at v = 4 m/s calculated for each station

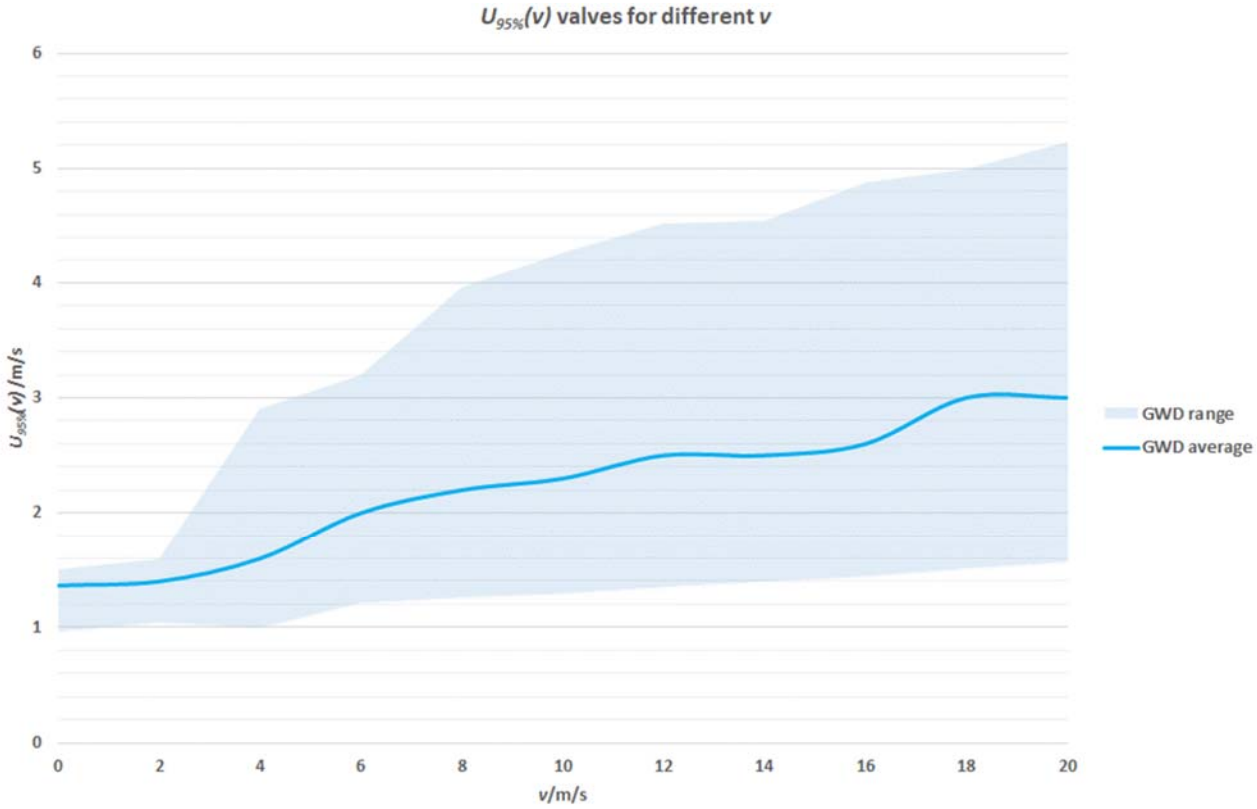

Fig. 7 Expanded measurement uncertainty $U_{95\%}(v)$ at various values of v (line chart - average measurement uncertainty; area graph - range of measurement uncertainties)

D. Solar Radiation

In Fig. 8 and 9, the expanded measurement uncertainty for solar radiation at 800 W/m² is presented. Fig. 8 illustrates the calculated uncertainty for each station, making the differences between the various locations apparent. Fig. 9 shows the measurement uncertainty across the entire measured area. The line on the graph represents the average uncertainty for solar radiation, derived from the uncertainties at all stations. The area chart highlights the range between the minimum and maximum uncertainties for individual solar radiation values.

IV. Discussion

In this study, we focused on the evaluation of the measurement uncertainty of meteorological parameters calculated with the diagnostic microscale meteorological model CALMET. Our results indicate that measurement uncertainty is non-negligible and can play a crucial role in processes, relying on precise forecasting.

Based on the calculation of combined measurement uncertainty for temperature, relative humidity, and solar radiation, it can be concluded that fluctuations in measurement uncertainty among different stations are not significant and are due to local factors. Also, the measurement uncertainty is constant across the entire measured range except for the values above 85% RH, where the derived higher measurement uncertainty can be explained with greater measurement uncertainty of the used measurement equipment in that range.

Higher measurement uncertainties for temperature are found at the stations located near forests (stations 26, 27, 29), which can be interpreted with proximity of trees affecting the temperature forecast or the possibility of errors inflicted by the specific placement of measurement equipment (shaded or sunlit side).

Calculations of measurement uncertainty for relative humidity range from 8 to 12% RH, except for the station located in a forest marked as 28. The cause of such high measurement uncertainty value was determined to be the malfunction of the capacitive humidity sensor. After the sensor was replaced at the end of 2022, the discrepancy between measured and predicted values decreased.

The high measurement uncertainty for solar radiation is due to the fact that measured values of solar radiation in full sunlight reach 1200 W/m², while the highest predicted values in the forecast stands at 900 W/m². Measurement uncertainty could be significantly reduced with a systematic approach to data analysis.

Measurement uncertainty for wind speed depends on the actual measured value and only increases with higher wind speeds. At lower speeds, it ranges between 1-2 m/s, and at higher wind speeds, it averages above 3 m/s. The scale of measurement uncertainty dependency from higher wind speed values is also reflected in Fig. 6, where at stations with higher average wind speeds, the calculated measurement uncertainty is also higher.

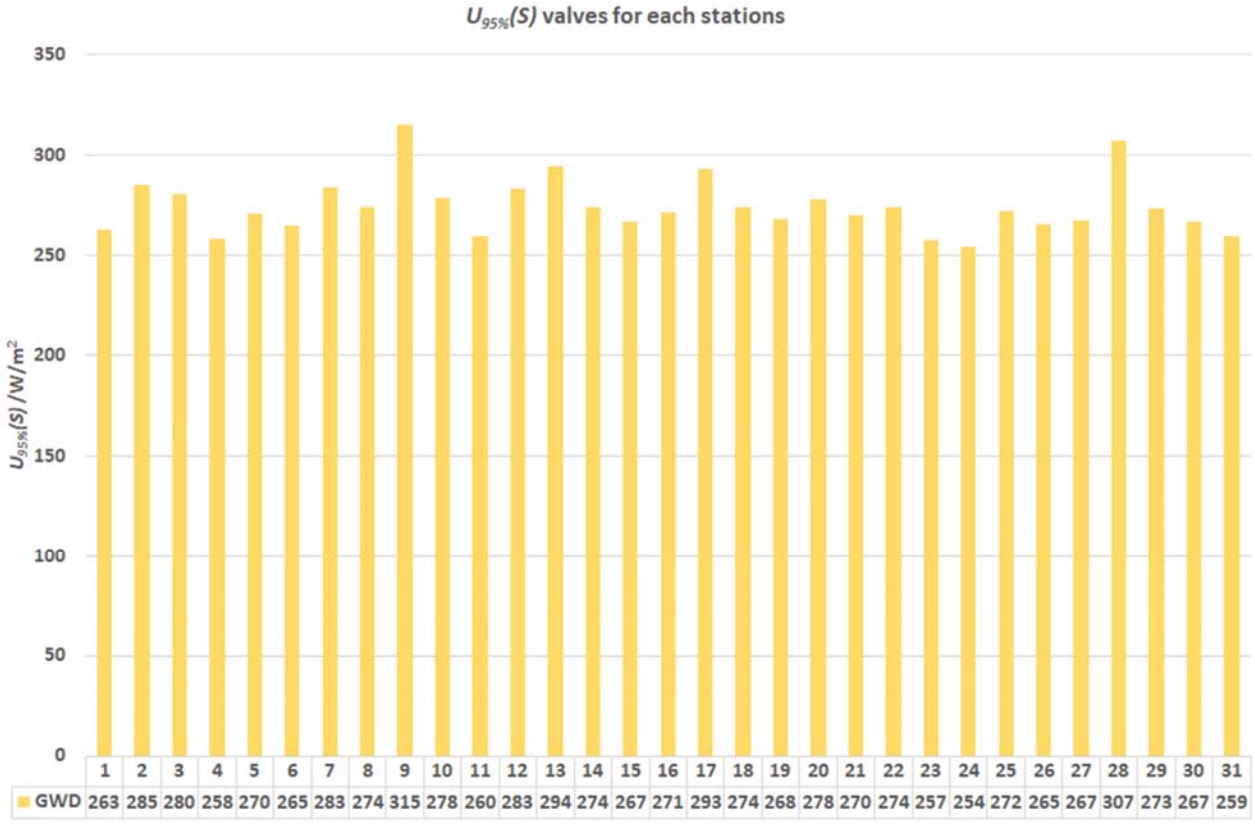

Fig. 8 Expanded measurement uncertainty $U_{95\%}(S)$ at S = 800 W/m^2 calculated for each station

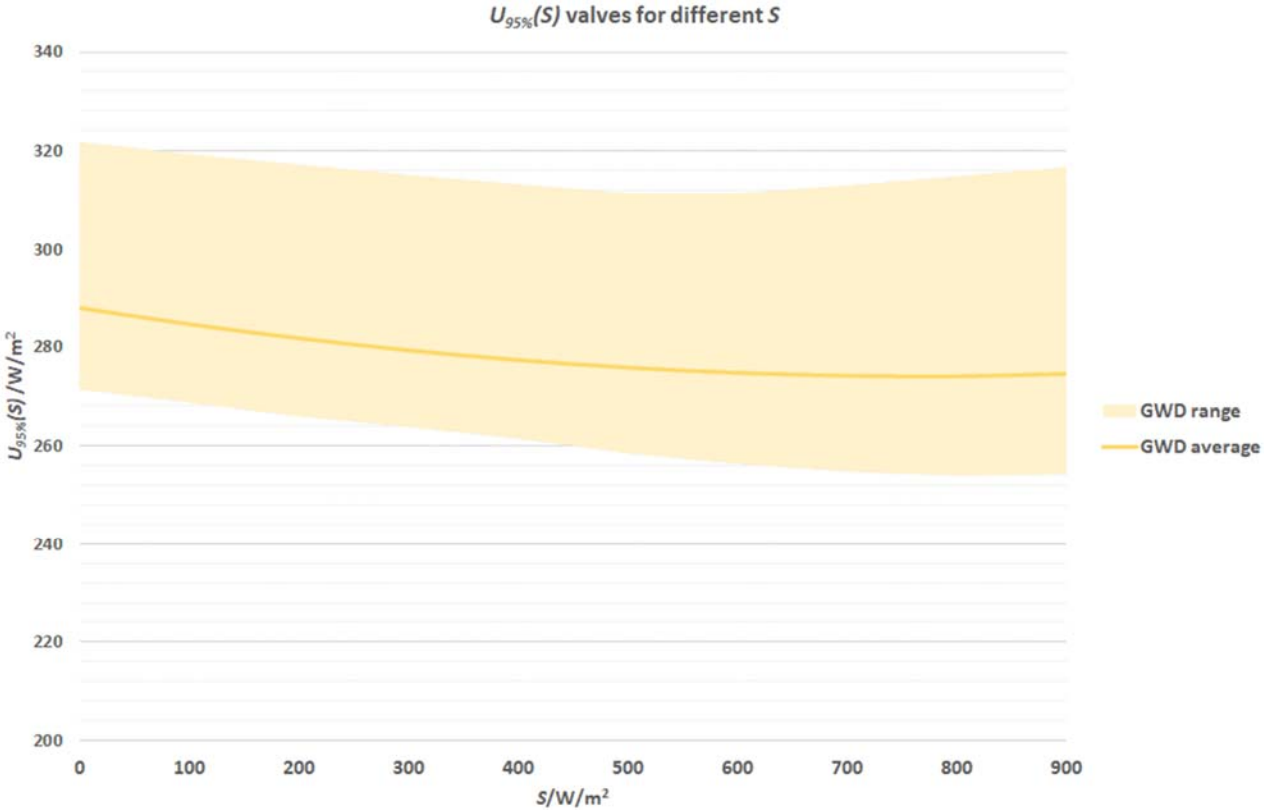

Fig. 9 Expanded measurement uncertainty $U_{95\%}(S)$ at various values of S (line chart - average measurement uncertainty; area graph - range of measurement uncertainties)

The final analysis of the presented graphs and data obtained from the CALMET model confirms that measurement uncertainty is of paramount importance in interpreting meteorological parameters. Differences in measurement uncertainty, reflecting various geographical, environmental, and technological conditions, were found to significantly affect the reliability and usability of meteorological forecasts.

Measurement uncertainty directly impacts the quality and credibility of forecasts, which is especially important in Slovenia, where weather forecasts are used by the distributors of electricity to predict the transmission of electrical current through power lines. Understanding and reducing measurement uncertainty enhances the ability to better manage natural resources, respond more effectively to natural disasters, and optimize agricultural and industrial processes. Based on the obtained results, it is recommended to apply additional safety measures and adjustments in planning and decision-making processes that rely on meteorological forecasts to reduce risks.

In this work, the importance of providing accurate and reliable weather data was emphasized, and it was demonstrated how the calculation of measurement uncertainty contributes to the greater quality and accuracy of weather models. As a result, it not only allows better interpretation of existing data, but also highlights the potential for further improvements in meteorological predictions. Future research should focus on improving measuring instruments and models to reduce measurement uncertainty. Additionally, new methods should be developed for better integration of data from different sources to enhance the accuracy of meteorological forecasts.

Finally, it must be emphasized that further development and improvement of meteorological measurement instruments and models will undoubtedly contribute to more accurate and reliable weather forecasts, which will have a broad spectrum of positive effects on many areas of human activity.

REFERENCES

[1] http://www.src.com/
[2] Scire, J.S., and Robe, F.R. "Fine-scale application of CALMET meteorological model to a complex terrain site," paper presented at the *Air & Waste Management Association 90th Annual Meeting and Exhibition*, 8-13 June 1997, Toronto, Canada.
[3] CALPUFF Modeling System Version 6 User Instructions, April 2011.
[4] https://esdac.jrc.ec.europa.eu/projects/srtmshuttle-radar-topogr
[5] https://www.e-prostor.gov.si/
[6] BIPM, JCGM 100:2008, "Evaluation of measurement data – Guide to the expression of uncertainty in measurement," Corrected version 2010.
[7] Keleş, T. "Comparison of Classical Least Squares and Orthogonal Regression in Measurement Error Models," *Journal of Educational Sciences*, 2018.
[8] CEN TC 264 WG 21. "Test protocol for field validation of B[a]P reference measurement methods," Working Group Document N67.
[9] Report by an EC Working Group on Guidance for the Demonstration of Equivalence, 2010.
[10] Vaisala, "User Guide, Vaisala Weather Transmitter WXT530 Series."
[11] Kipp & Zonen, "Operational Manual, SMP Series Smart Pyranometers."
[12] Calibration sheet no. H31-19450037.
[13] Calibration certificate Kipp & Zonen 019643190529.